Investigation of anisotropic velocity distribution functions using numerical solutions of the stationary Vlasov equation

gabi@venus.nipne.ro

Gabriel Voitcu[1], Costel Bunescu[1], Marius M. Echim[1,2]

[1]Institute for Space Sciences, Magurele, Romania; [2]Belgian Institute for Space Aeronomy, Bruxelles, Belgium

1 Numerical model

$$\frac{\partial f}{\partial t}+\vec{v}\cdot\frac{\partial f}{\partial \vec{r}}+\frac{q}{m}(\vec{E}+\vec{v}\times\vec{B})\cdot\frac{\partial f}{\partial \vec{v}}=0$$

in the stationary case the characteristics of the Vlasov equation are given by

$t_0=0$ $\qquad$ $t>t_0$

$$\mathcal{R}_o=\begin{pmatrix} x_0^1 & y_0^1 & z_0^1\\ \vdots & \vdots & \vdots\\ x_0^N & y_0^N & z_0^N\end{pmatrix} \qquad \mathcal{V}_o=\begin{pmatrix} v_{0x}^1 & v_{0y}^1 & v_{0z}^1\\ \vdots & \vdots & \vdots\\ v_{0x}^N & v_{0y}^N & v_{0z}^N\end{pmatrix}$$

$$\frac{d^2\vec{r}}{dt^2}=\frac{q}{m}\left(\vec{E}+\frac{d\vec{r}}{dt}\times\vec{B}\right)$$

$$\mathcal{R}=\begin{pmatrix} x^1 & y^1 & z^1\\ \vdots & \vdots & \vdots\\ x^N & y^N & z^N\end{pmatrix} \qquad \mathcal{V}=\begin{pmatrix} v_x^1 & v_y^1 & v_z^1\\ \vdots & \vdots & \vdots\\ v_x^N & v_y^N & v_z^N\end{pmatrix}$$

$$f_0(v_x,v_y,v_z)=n_0\left(\frac{m}{2\pi kT_0}\right)^{3/2} e^{-\frac{m\left[(v_x-V_0)^2+v_y^2+v_z^2\right]}{2kT_0}}$$

$$\vec{B}(x)=\frac{\vec{B}_1}{2}erfc\left(\frac{x}{L}\right)+\frac{\vec{B}_2}{2}\left[2-erfc\left(\frac{x}{L}\right)\right]$$

$$\vec{E}(x)=\vec{B}(x)\times\vec{U}_E,\quad \vec{U}_E=const.$$

$$f(\vec{r},\vec{v})\ -\ VDF\ at\ the\ end\ of\ simulation$$

$$\mathcal{F}=(f_0^1,f_0^2,\ldots,f_0^N)$$

along a particle trajectory df/dt=0

$$\mathcal{F}=(f_0^1,f_0^2,\ldots,f_0^N)$$

2 Input parameters

	N_0 (m^{-3})	T_0 (keV)	V_0 (km/s)	B_{1z} (nT)	B_{2z} (nT)	L (km)	Nx, Ny	nps	x_0, y_0 (km)	dx_0, dy_0 (km)
H^+	10^4	7	200	-30	30, 60	6000	12, 12	75000	-20000, -1100	200, 200

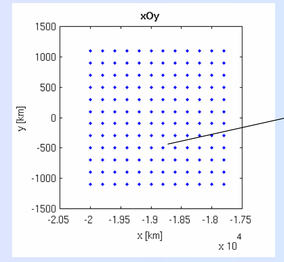

The position of all 144 sources of protons in the xOy plane. 75000 test-particles are injected from each source.

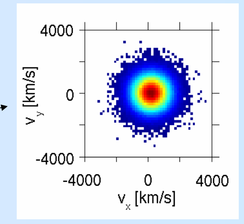

The initial velocity distribution function (VDF) of protons is described by a displaced Maxwellian for each source.

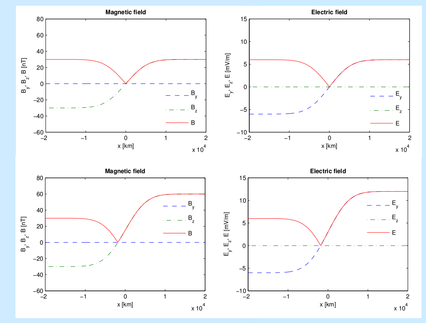

The magnetic filed distribution (left plot) and the electric filed distribution (right plot) in the simulation domain. Top panels correspond to case A (B_{2z}=30nT) and bottom panels correspond to case B (B_{2z}=60nT).

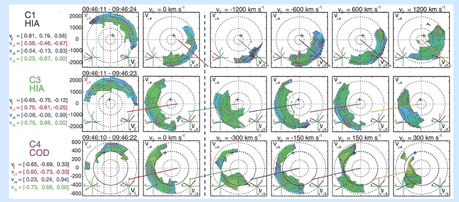

The velocity distribution function of ions experimentally observed by CLUSTER-1 (top) and CLUSTER-3 (bottem) satellites in the terrestrial magnetotail, at 18R_E, on 1 October 2001 (Wilber et al., 2004).

3 Results

t=10s

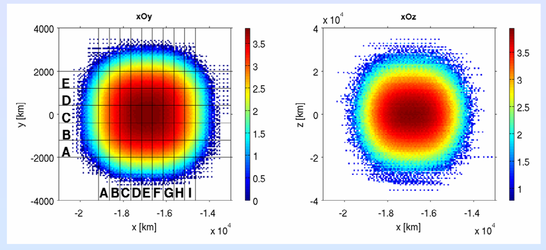

Figure 1 - The position of protons in the xOy and xOz planes obtained at the end of the simulation. Local value of the number density is color coded. The spatial mesh on which the VDF is reconstructed is also shown.

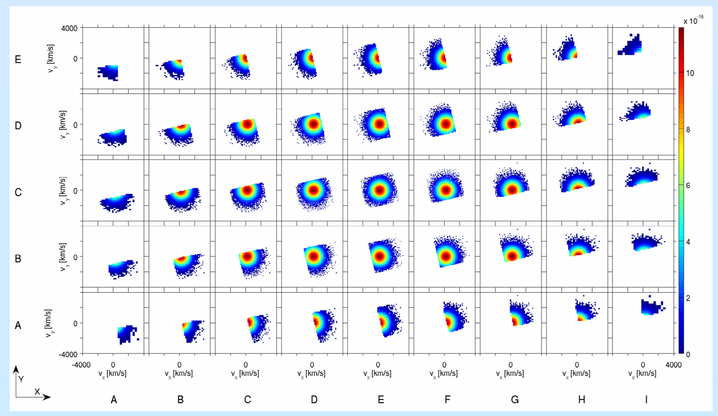

Figure 2 - Kinetic structure of the proton cloud. The spatial variation of the VDF of protons is shown for the mesh defined in figure 1. Note that in the central region of the cloud the VDF remain a displaced Maxwelian.

Case A
t=180s

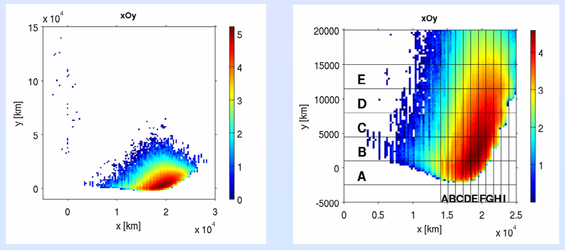

Figure 3 - The position of protons in the xOy plane obtained at the end of the simulation. Local value of the number density is color coded. The spatial mesh on which the VDF is reconstructed is also shown.

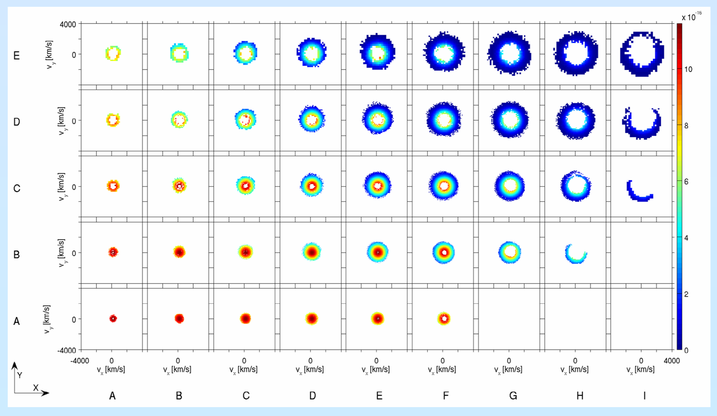

Figure 4 - Kinetic structure of the proton cloud. The spatial variation of the VDF of protons is shown for the mesh defined in figure 3. Note the formation of a cavity in the central region of the VDF.

Case B
t=180s

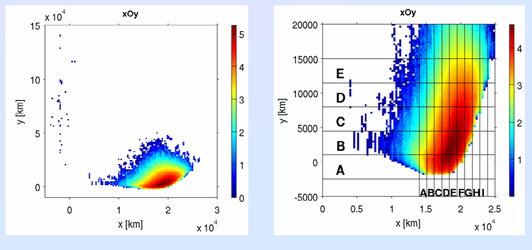

Figure 5 - The position of protons in the xOy plane obtained at the end of the simulation. Local value of the number density is color coded. The spatial mesh on which the VDF is reconstructed is also shown.

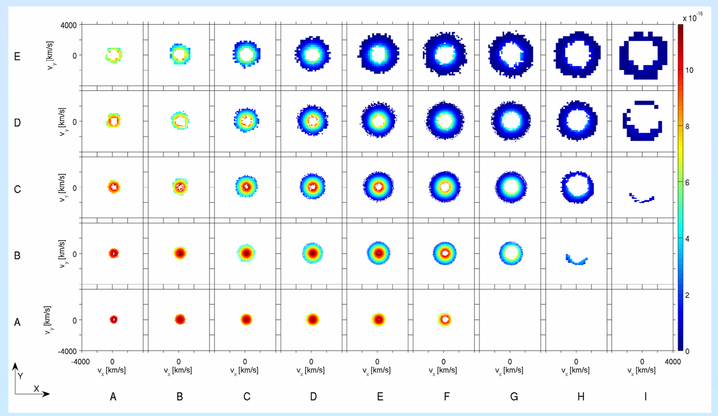

Figure 6 - Kinetic structure of the proton cloud. The spatial variation of the VDF of protons is shown for the mesh defined in figure 5. Note that the dimensions of the cavity are larger when the magnetic field increases.

4 Discussion and Conclusions

The results show that the proton cloud penetrates the transition region and moves into the "right hand side" domain. The dynamics of the proton cloud reveals asymmetries for both values of the asymptotic magnetic field. The protons are scattered in the positive direction of the y-axis. The asymmetric expansion of the cloud is due to the positive gradient-B drift, acting in the discontinuity region. It can be seen that the spatial scattering of the protons varies inverse proportionally with the asymptotic value of the magnetic field. This confirms the role of the gradient-B drift that varies proportionally with $|gradB|/B^2$. On the other hand, the Larmor radius varies inverse proportionally with the magnetic induction such that the proton cloud dimensions in the xOy plane are smaller for a larger value of the asymptotic magnetic field intensity. The results shows an interesting property of the VDF: the formation of a cavity region in the central part of the VDF. This kinetic effect is observed in spatial regions close to the lateral wings of the cloud. The area of the cavity formed in the space of perpendicular velocities varies with the distance from the center of the cloud. It is thus suggested that the edges of the cloud are mainly populated by the most energetic particles of the initial velocity distribution. Since everywhere E is perpendicular to B, there is no electrostatic acceleration. We conjecture that the physical mechanism that introduces this anisotropy of the VDF is related to the expansion of the cloud in the +Oy direction. It is thus a finite Larmor effect due to the gradient-B drift. The anisotropy observed in the front-side region is a non-local effect which we associate to the remote sensing of particles whose guiding centers pertain to the inner cloud. Similar conjectures have been made by Lee et al. (2004) for in-situ data recorded in the magnetospheric tail, but these authors did not explain the formation of the cavity itself.

5 References & Aknowledgments

[1] T. W. Speiser, J. Geophys. Res. 70, 4219 (1965).
[2] T. W. Speiser, J. Geophys. Res. 72, 3919 (1967).
[3] J. W. Eastwood, Planet. Space Sci. 20, 1555 (1972).
[4] J. W. Eastwood, Planet. Space Sci. 23, 1 (1975).
[5] K. D. Cole, Planet. Space Sci. 24, 515 (1976).
[6] K. D. Cole, Phys. Plasmas 3, 2717 (1996).
[7] P. L. Rothwell, M. B. Silevich, L. P. Block, C. G. Falthammar, J. Geophys. Res. 100, 14875 (1995).
[8] M. M. Echim, Cosmic Research 40, 534 (2002).
[9] T. W. Speiser, D. J. Williams, H. A. Garcia, J. Geophys. Res. 86, 723 (1981).
[10] L. R. Lyons, T. W. Speiser, J. Geophys. Res. 87, 2276 (1982).
[11] D. J. Williams, T. W. Speiser, J. Geophys. Res. 89, 8877 (1984).
[12] D. B. Curran, C. K. Goertz, T. A. Whelan, Geophys. Res. Lett. 14, 99 (1987).
[13] D. B. Curran, C. K. Goertz, J. Geophys. Res. 94 (1989).
[14] S. Chandrasekhar, Plasma Physics, University of Chicago Press (1960).
[15] J. L. Delcroix, A. Bers, Physique des plasmas, Savoirs Actuels-InterÉditions/CNRS Éditions, Paris (1994).
[16] A. Sestero, Phys. Fluids 7, 44 (1964).
[17] J. Lemaire, L. F. Burlaga, Astrophys. Space Sci. 45, 303 (1976).
[18] M. Roth, J. DeKeyser, M. M. Kuznetsova, Space Science Reviews 76, 251 (1996).
[19] G. Schmidt, Phys. Fluids 3, 961 (1960).
[20] M. Galvez, G. Gisler, C. Barnes, Phys. Fluids B 2(3), 516 (1990).
[21] D. S. Cai, O. Buneman, Phys. Fluids B 4(4), 1033 (1992).
[22] M. Wilber et al., Geophys. Res. Lett. 31, (2004).
[23] E. Lee et al., Geophys. Res. Lett. 31, (2004).

Work supported by ESA PECS contract 98089 and ANCS contract SAFIR (81-009).